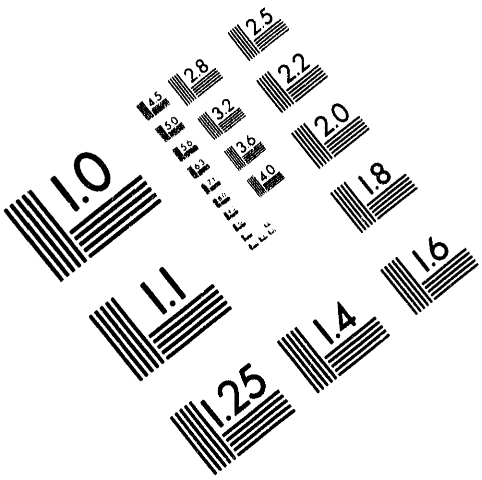

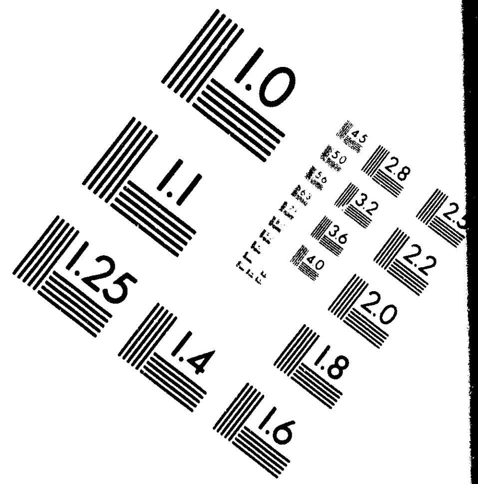

AIIM

Association for Information and Image Management

1100 Wayne Avenue, Suite 1100
Silver Spring, Maryland 20910
301/587-8202

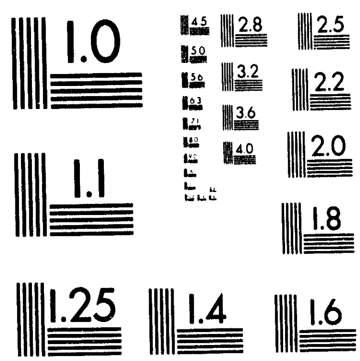

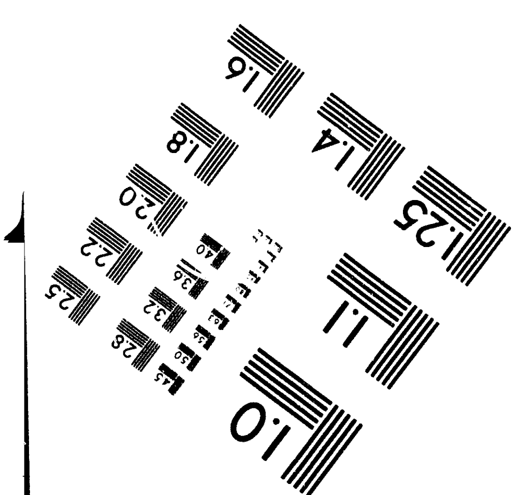

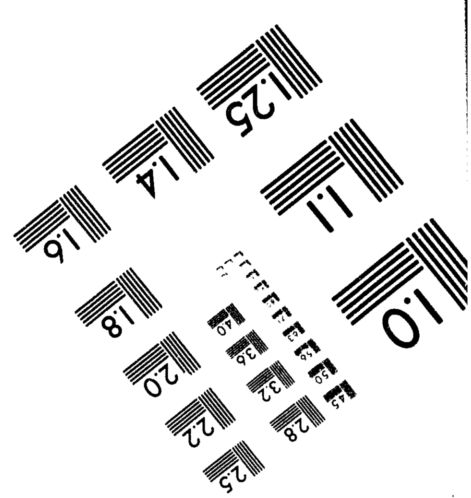

MANUFACTURED TO AIIM STANDARDS
BY APPLIED IMAGE, INC.

SC-MAG-464
LBL—35928

Magnetic Field Components in a Sinusoidally Varying Helical Wiggler.*

Shlomo Caspi

Lawrence Berkeley Laboratory
University Of California
Berkeley, CA 94720

July 27, 1994

* This was supported by the Director, Office of Energy Research, Office of High Energy and Nuclear Physics, High Energy Physics Division, U. S. Department of Energy, under Contract No. DE-AC03-76SF00098.

Abstract

One may be interested in a pure multipole magnetic field (i.e, proportional to sin(nθ) or cos(nθ)) whose strength varies purely as a Fourier sinusoidal series of the longitudinal coordinate z (say proportional to cos $\frac{(2m-1)\pi z}{L}$, where L denotes the *half-period* of the wiggler and m=1,2,3 ...). Associated with such a z variation, there necessarily will be present a z component of magnetic field which in the source-free region, in fact, will give rise to both normal and skew transverse fields associated with the functions $A_n(z)$ *and* $\tilde{A}_n(z)$ as expressed in Reference[bc]. In this note the field components and expression for the scalar potential both inside and outside a thin pure winding surface are included with additional contributions from a possible high permeable shield. It is also shown that for a pure dipole case of n=1 and a pure axial variation of m=1 the transverse field can be derived from a simple two dimensional field.

Scalar Potential

We note that in the curl-free divergence-free region near the axis r=0 the field components may be expressed as given by $\vec{B} = -\nabla V$ where V is a scalar potential function for which $\nabla^2 V = 0$.

$$\frac{1}{r}\frac{\partial}{\partial r}\left(r\frac{\partial V}{\partial r}\right) + \frac{\partial^2 V}{\partial z^2} - \frac{n^2 V}{r^2} = 0 \tag{1}$$

The general form for the proposed solution as shown in Reference c can be written in the form that includes both "skew" and "non-skew" terms of all integer harmonic of order n (*including n=0*):

$$V = -\left\{\sum_{n=0} r^n \sum_{k=0} \frac{(-1)^{k+1} n!}{2^{2k} k!(n+k)!}\, r^{2k} \left[A_n^{(2k)}(z)\sin n\theta - \tilde{A}_n^{(2k)}(z)\cos n\theta\right]\right\} \tag{2}$$

and the magnetic field components derived accordingly as :

$$\begin{aligned} B_r &= -\frac{\partial V}{\partial r} = \sum_n \left[g_{rn} r^{n-1}\sin n\theta - \tilde{g}_{rn} r^{n-1}\cos n\theta\right] \\ B_\theta &= -\frac{n}{r}V = \sum_n \left[g_{\theta n} r^{n-1}\cos n\theta + \tilde{g}_{\theta n} r^{n-1}\sin n\theta\right] \\ B_z &= -\frac{\partial V}{\partial z} = \sum_n \left[g_{zn} r^{n}\sin n\theta - \tilde{g}_{zn} r^{n}\cos n\theta\right] \end{aligned} \tag{3}$$

where

$$\begin{aligned} g_{rn} &\equiv \tilde{g}_{rn} \\ g_{\theta n} &\equiv \tilde{g}_{\theta n} \\ g_{zn} &\equiv \tilde{g}_{zn} \end{aligned} \tag{4}$$

are general functions of r and z that include the appropriate "normal" and "skew" terms $A_n(z)$ *and* $\tilde{A}_n(z)$ (see Appendix B).

---

[b] 3D Field Harmonics — S.Caspi , M.Helm , and L.J. Laslett , SC-MAG-328 , LBL-30313 , March 1991.

[c] An Approach To 3D Magnetic Field Calculation Using Numerical and Differential Algebra Methods — S.Caspi , M.Helm , and L.J. Laslett , SC-MAG-395 , LBL-32624 , July 1992.

Inner Field r < R

For the region within the windings (R equals the thin winding radius) of a helical wiggler such functions and even derivatives of order (2k) are expressed as

$$
\begin{aligned}
A_n(z) &= \sum_{m=1} B_{n,m} \cos\left[(2m-1)\frac{\pi z}{L}\right] \\
\tilde{A}_n(z) &= \sum_{m=1} B_{n,m} \sin\left[(2m-1)\frac{\pi z}{L}\right] \\
A_n^{(2k)}(z) &= \sum_{m=1} (-1)^k \left[\frac{(2m-1)\pi}{L}\right]^{2k} B_{n,m} \cos\left[(2m-1)\frac{\pi z}{L}\right] \\
\tilde{A}_n^{(2k)}(z) &= \sum_{m=1} (-1)^k \left[\frac{(2m-1)\pi}{L}\right]^{2k} B_{n,m} \sin\left[(2m-1)\frac{\pi z}{L}\right]
\end{aligned} \tag{5}
$$

and with the substitution of the above expressions into the scalar potential V (Equation 2)

$$
V(r,\theta,z) = \sum_{n=1} n! \sum_{m=1} B_{n,m} \left[\frac{2L}{(2m-1)\pi}\right]^n \sum_{k=0} \frac{1}{k!(n+k)!} \left[\frac{(2m-1)\pi r}{2L}\right]^{2k+n} \sin\left[n\theta - \frac{(2m-1)\pi z}{L}\right] \tag{6}
$$

and with

$$
I_n(\omega_m r) = \sum_{k=0} \frac{1}{k!(n+k)!} \left(\frac{\omega_m r}{2}\right)^{2k+n} \tag{7}
$$

where I_n denotes the "modified" Bessel function (of the first kind and order n),

$$
\omega_m = \frac{(2m-1)\pi}{L} \qquad and \qquad G_{n,m} = n!\left(\frac{2}{\omega_m}\right)^n B_{n,m} \tag{8}
$$

we express the scalar potential (Equation 6) as

$$
V(r,\theta,z) = \sum_{n=1} \sum_{m=1} G_{n,m} I_n(\omega_m r) \sin(n\theta - \omega_m z) \tag{9}
$$

where for a dipole sextupole , decapole etc, n=1,3,5...., m=1,2,3...., and L = half period.

The transverse field components and z directed field thus become

$$
\begin{aligned}
B_r &= -\frac{\partial V}{\partial r} = -\sum_{n=1} \sum_{m=1} G_{n,m} \omega_m I_n'(\omega_m r) \sin(n\theta - \omega_m z) \\
B_\theta &= -\frac{1}{r}\frac{\partial V}{\partial \theta} = -\sum_{n=1} \sum_{m=1} n G_{n,m} \frac{1}{r} I_n(\omega_m r) \cos(n\theta - \omega_m z) \\
B_z &= -\frac{\partial V}{\partial z} = \sum_{n=1} \sum_{m=1} G_{n,m} \omega_m I_n(\omega_m r) \cos(n\theta - \omega_m z)
\end{aligned} \tag{10}
$$

with

$$
I_n'(\omega_m r) = I_{n-1}(\omega_m r) - \frac{n}{\omega_m r} I_n(\omega_m r) \tag{11}
$$

where the prime denotes differentiation of the Bessel function with respect to its argument.

Outer Field r > R

For a configuration in which the magnetic field components are produced by means of currents confined to lie on the surface of a circular cylinder (radius R), it can be of interest to evaluate the character of the magnetic field components that must be present in the external region (r>R) and to determine the components (J_z and J_θ, at R) of current density for this configuration. The surface currents will give rise to a discontinuity of the components B_z and B_θ at the interface (r=R), but the normal (radial) component will pass continuously through this surface and assume the form

$$B_r = -\sum_{n=1}\sum_{m=1} G_{n,m}\omega_m \frac{I_n'(\omega_m R)}{K_n'(\omega_m R)} K_n'(\omega_m r) \sin(n\theta - \omega_m z) \qquad (for \;\; r \geq R) \qquad (12)$$

Consistent with B_r written immediately above a scalar potential function V for the external region is given by

$$V = \sum_{n=1}\sum_{m=1} G_{n,m} \frac{I_n'(\omega_m R)}{K_n'(\omega_m R)} K_n(\omega_m r) \sin(n\theta - \omega_m z) \qquad (for \;\; r \geq R) \qquad (13)$$

where the prime denotes differentiation of the Bessel functions with respect to its argument, and

$$K_n'(\omega_m r) = -\left[K_{n-1}(\omega_m r) + \frac{n}{\omega_m r} K_n(\omega_m r)\right] \qquad (14)$$

The remaining field components are found to be

$$\begin{aligned} B_\theta &= -\sum_{n=1}\sum_{m=1} nG_{n,m} \frac{I_n'(\omega_m R)}{K_n'(\omega_m R)} \frac{1}{r} K_n(\omega_m r) \cos(n\theta - \omega_m z) \\ B_z &= \sum_{n=1}\sum_{m=1} G_{n,m}\omega_m \frac{I_n'(\omega_m R)}{K_n'(\omega_m R)} K_n(\omega_m r) \cos(n\theta - \omega_m z) \end{aligned} \qquad (15)$$

Surface currents at r=R

The discontinuity of the field components at the interface r=R now permit evaluation of the corresponding surface currents on this cylindrical surface. We denote the current system at the interface r=R by $\vec{J} = J_z \hat{e}_z + J_\theta \hat{e}_\theta$ (amp/m), and recall the relation $\frac{1}{\mu_0} \oint \vec{B} \cdot dl = I$ (or $\frac{1}{\mu_0}(\Delta B) = J$), where $\mu_0 = 4\pi 10^{-7}$ in MKS-A units. Then

$$\begin{aligned} J_z(\theta, z)|_{r=R} &= \frac{1}{\mu_0}\left[B_\theta^{ext.} - B_\theta^{int.}\right] \\ &= \frac{1}{\mu_0} \sum_{n=1}\sum_{m=1} nG_{n,m} \frac{I_n(\omega_m R)K_n'(\omega_m R) - I_n'(\omega_m R)K_n(\omega_m R)}{RK_n'(\omega_m R)} \cos(n\theta - \omega_m z) \end{aligned} \qquad (16)$$

and through the use of the Wronskian $I_n K_n' - I_n' K_n = -\frac{1}{\omega_m R}$

$$J_z(\theta, z)|_{r=R} = -\frac{1}{\mu_0} \sum_{n=1}\sum_{m=1} nG_{n,m} \frac{1}{\omega_m R^2} \frac{1}{K_n'(\omega_m R)} \cos(n\theta - \omega_m z) \qquad (17)$$

and

$$J_\theta(\theta,z)|_{r=R} = \frac{1}{\mu_0}\left[B_z^{int.} - B_z^{ext.}\right]$$
$$= \frac{1}{\mu_0}\sum_{n=1}\sum_{m=1} G_{n,m}\omega_m \frac{I_n(\omega_m R)K_n'(\omega_m R) - I_n'(\omega_m R)K_n(\omega_m R)}{K_n'(\omega_m R)}\cos(n\theta - \omega_m z) \tag{18}$$

and again through the use of the Wronskian

$$J_\theta(\theta,z)|_{r=R} = -\frac{1}{\mu_0}\sum_{n=1}\sum_{m=1} G_{n,m}\frac{1}{R}\frac{1}{K_n'(\omega_m R)}\cos(n\theta - \omega_m z) \tag{19}$$

The pair of components satisfy the conservation condition $\nabla \cdot \vec{J} = \frac{\partial J_z}{\partial z} + \frac{1}{R}\frac{\partial J_\theta}{\partial \theta} = 0$ as required.

Contribution of axially-symmetric ferromagnetic shield

We realize that if an axially-symmetric ferromagnetic shield of high permeability is present with a radius r=a (a > R), the induced magnetization will contribute supplemental fields ("image fields") that in the region interior to r=a may themselves be derived from a scalar potential ($V_{r<a}^{image}$). The appropriate boundary condition at r=a will be fulfilled if we specify that $V_{r=a}^{image} + V_{r=a}^{direct} = constant$ or if we conveniently specify that $V_{r=a}^{image} = -V_{r=a}^{direct}$ and specifically

$$V_{r=a}^{image} = -\sum_{n=1}\sum_{m=1} G_{n,m}\frac{I_n'(\omega_m R)}{K_n'(\omega_m R)}K_n(\omega_m a)\sin(n\theta - \omega_m z) \qquad (at\ r = a) \tag{20}$$

If the iron radius is constant (not a function of z) we can write the scalar potential for r≤a

$$V^{image} = -\sum_{n=1}\sum_{m=1} G_{n,m}\frac{I_n'(\omega_m R)K_n(\omega_m a)}{K_n'(\omega_m R)I_n(\omega_m a)}I_n(\omega_m r)\sin(n\theta - \omega_m z) \qquad (at\ r \le a) \tag{21}$$

For the TOTAL magnetic potential function at r<R<a , we then have

$$V_{r<R}^{total} = \sum_{n=1}\sum_{m=1} G_{n,m}\left[1 - \frac{I_n'(\omega_m R)K_n(\omega_m a)}{K_n'(\omega_m R)I_n(\omega_m a)}\right]I_n(\omega_m r)\sin(n\theta - \omega_m z) \tag{22}$$

The factor contained within the square brackets is an enhancement factor arising from the inclusion of magnetization developed in the high permeability ferromagnetic shield. For the special 2d case where $L \to \infty$ or ω_ma<<1 this factor becomes approximately

$$lim_{\omega_m a \to 0}\left[1 - \frac{I_n'(\omega_m R)K_n(\omega_m a)}{K_n'(\omega_m R)I_n(\omega_m a)}\right] = 1 + \left(\frac{R}{a}\right)^{2n} \tag{23}$$

and the potential

$$V_{r<R}^{total-2D} \approx \sum_{n=1}\sum_{m=1} B_{n,m}\left[1 + \left(\frac{R}{a}\right)^{2n}\right]r^n\sin(n\theta - \omega_m z) \tag{24}$$

as expected for the enhancement of the 2D field. For the above approximation we made use of the following asymptotic relations

$$\begin{aligned} & s \rightarrow 0 \\ & I_n(s) \sim \frac{1}{n!}\left(\frac{s}{2}\right)^n \\ & K_n(s) \sim \frac{(n-1)!}{2}\left(\frac{s}{2}\right)^{-n} \\ & I_n'(s) \sim \frac{1}{2(n-1)!}\left(\frac{s}{2}\right)^{n-1} \\ & K_n'(s) \sim -\frac{n!}{4}\left(\frac{s}{2}\right)^{-(n+1)} \end{aligned} \tag{25}$$

The square brackets in Equation (22) is plotted in Fig. 4 Appendix A for n=1 and m=1.

Helical dipole with simple sinusoidal relation

We shall examine a helical dipole with single terms for both series n and m. The choice n=1 indicates a pure dipole with no higher harmonics , and m=1 indicates a pure $\pi z/L$ variation with no additional frequencies. We express the field components for r<R and n=m=1 as

$$\begin{aligned} & \omega_m = \omega_1 = \frac{\pi}{L} \quad , \quad G_{n,m} = G_{1,1} = \frac{2L}{\pi} B_{1,1} \\ & B_r = -2B_{1,1} I_1'\left(\frac{\pi r}{L}\right) \sin\left(\theta - \frac{\pi z}{L}\right) \\ & B_\theta = -2B_{1,1}\left(\frac{L}{\pi r}\right) I_1\left(\frac{\pi r}{L}\right) \cos\left(\theta - \frac{\pi z}{L}\right) \\ & B_z = 2B_{1,1} I_1\left(\frac{\pi r}{L}\right) \cos\left(\theta - \frac{\pi z}{L}\right) \end{aligned} \tag{26}$$

and

$$\vec{J}(\theta, z) = -\frac{2B_{1,1}}{\mu_0}\left(\frac{L}{\pi R}\right)\frac{1}{K_1'(\frac{\pi R}{L})}\left[\hat{e}_\theta + \frac{L}{\pi R}\hat{e}_z\right] \cos\left(\theta - \frac{\pi z}{L}\right) \tag{27}$$

We note that a linear relationship exists between the following field components

$$\frac{B_z}{B_\theta} = -\frac{\pi r}{L} \tag{28}$$

and note as well that for $\frac{\pi r}{L} < \frac{\pi}{2}$ *or* $r < \frac{L}{2}$ the field components can be expressed with less than 1% error as

$$\begin{aligned} B_r &= -B_{1,1}\left[1 + \frac{3}{2}\left(\frac{\pi r}{2L}\right)^2 + \frac{5}{12}\left(\frac{\pi r}{2L}\right)^4 + \frac{7}{144}\left(\frac{\pi r}{2L}\right)^6 + \cdots\right] \sin\left(\theta - \frac{\pi z}{L}\right) \\ B_\theta &= -B_{1,1}\left[1 + \frac{1}{2}\left(\frac{\pi r}{2L}\right)^2 + \frac{1}{12}\left(\frac{\pi r}{2L}\right)^4 + \frac{1}{144}\left(\frac{\pi r}{2L}\right)^6 + \cdots\right] \cos\left(\theta - \frac{\pi z}{L}\right) \\ B_z &= B_{1,1}\frac{\pi r}{L}\left[1 + \frac{1}{2}\left(\frac{\pi r}{2L}\right)^2 + \frac{1}{12}\left(\frac{\pi r}{2L}\right)^4 + \frac{1}{144}\left(\frac{\pi r}{2L}\right)^6 + \cdots\right] \cos\left(\theta - \frac{\pi z}{L}\right) \end{aligned} \tag{29}$$

The representations above will describe a field that formally is both divergence free and curl free — provided that the summations are not truncated. If, however, we wish to truncate these series expressions, we at best can only do so in such a way that one, but not both, of these conditions is satisfied. Thus, if we wish to preserve the divergence condition $\nabla \cdot \vec{B} = 0$, we should take care that the sum over the k index in the series for B_z should terminate at a value of k that is less by unity than the termination value for this index in the series for the transverse field components B_r & B_θ.

We shall calculate $B_{1,1}$ and compare it with B_{2d} that is produced by a straight long dipole ($L \to \infty$) carrying the same total current. In the 2D case where a current density (per unit length) of $J(\theta) = J_0 \cos\theta$ and $J_0 = \frac{I_0}{R}$ will produce a dipole field of $B_{2d} = \frac{\mu_0 J_0}{2}$, the dipole field in terms of the total amp-turn is

$$B_{2d} = \frac{\mu_0 I_0}{2R} \tag{30}$$

We shall evaluate the total amp-turn in the helical wiggler by integrating the azimuthal current density along θ=0 using equation (27) (see Fig. 1 below).

$$s = \frac{\pi R}{L}$$

$$I_0 = \int_0^{\frac{\pi}{2}} J_z|_{z=0} R d\theta = \int_0^{\frac{L}{2}} J_\theta|_{\theta=0} dz = -\frac{2B_{1,1}}{\mu_0}\frac{1}{sK_1'(s)}\int_0^{\frac{L}{2}} \cos\frac{\pi z}{L} dz = -\frac{2B_{1,1}R}{\mu_0 s^2 K_1'(s)} \tag{31}$$

By equating the total current in both the 2D dipole and the helical wiggler the ratio of their transverse fields can be reduced to a dimensionless form :

$$\frac{B_{1,1}}{B_{2d}} = s^2 K_1'(s) \tag{32}$$

and note that in the limiting case (using Eq. 25) as $L \to \infty$

$$lim_{s\to 0}\frac{B_{1,1}}{B_{2d}} = 1 \tag{33}$$

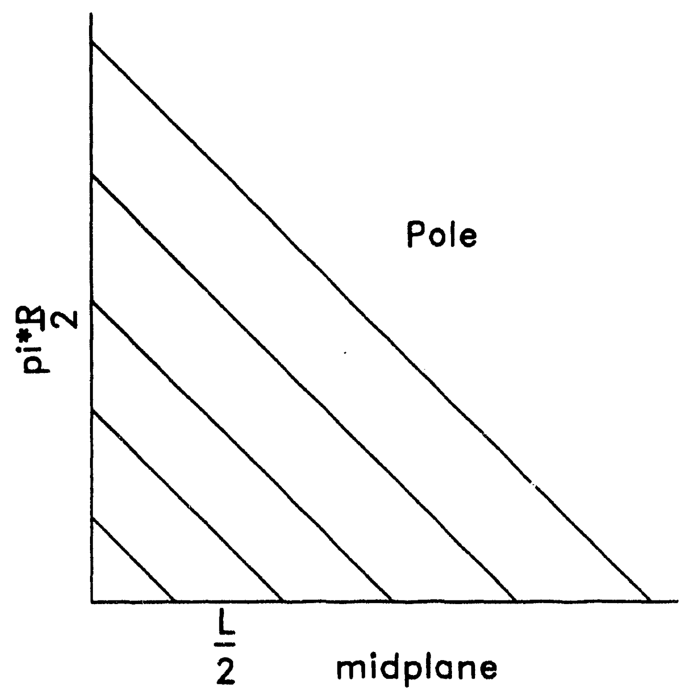

as it should be.

The relation between the normalized transverse fields and s (Eq. 32) plotted in Figure 1, reveals a range that surprisingly is grater than 1 where a maximum of 1.0616089 is reached at s=0.6 . A computational check was made with a cylinder of radius R=2.0 cm, surrounded by a current sheet in

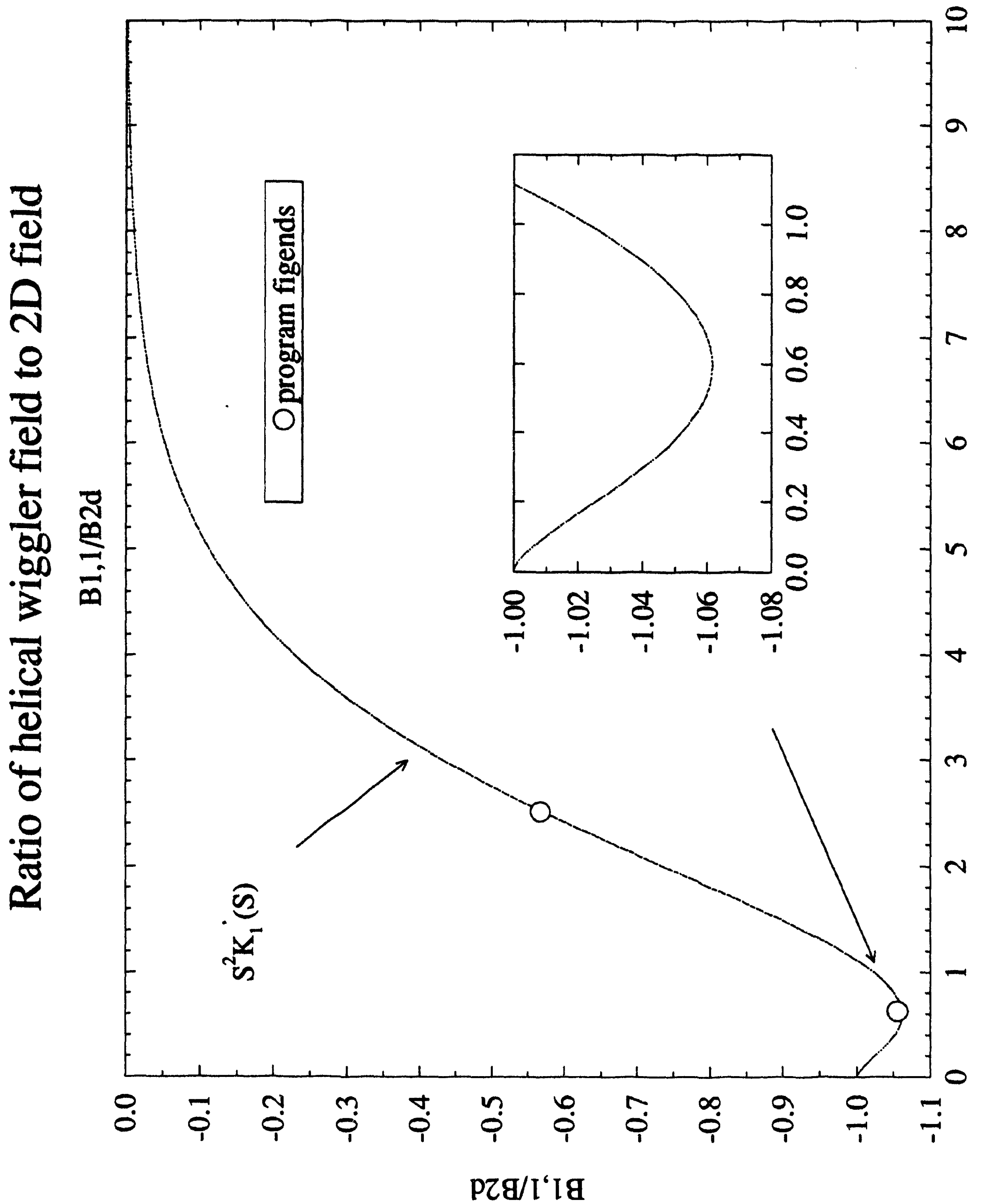

Figure 1 Ratio of wiggler field to 2d dipole field.

a cosθ fashion (Figure 2) such that

$$J = \frac{I_0}{R}\cos\theta = 39 \times 10^3 \cos\theta \quad (A/cm) \tag{34}$$

with a dipole field of

$$B_{2d} = \frac{\mu_0 I_0}{2R} = 2.4504 \ \ (tesla) \tag{35}$$

(we picked N=39 turns, I=2000 A and note that I_0=NI). A quick check with the 2D program "pkpeak" yields a similar value of B_{2d}=2.4583 (tesla). Applying the same current configuration in two examples of a helical wiggler with the same radius R but different periods, such that

$$\begin{aligned} \lambda_1 = 2L = 5 \quad cm \quad &, \quad s = \frac{\pi R}{L} = 2.513 \\ \lambda_2 = 2L = 20 \quad cm \quad &, \quad s = \frac{\pi R}{L} = 0.6283 \end{aligned} \tag{36}$$

Equation (32) then predicts the following results :

$$\frac{B_{1,1}(\lambda_1)}{B_{2d}} = 0.567 \qquad or \qquad B_{1,1} = 1.3976 \ \ (tesla)$$
$$\frac{B_{1,1}(\lambda_2)}{B_{2d}} = 1.06135 \qquad or \qquad B_{1,1} = 2.600 \ \ (tesla)$$

With the aid of the 3D program "figends" using a model such as shown in Figure 3, the corresponding values are :

$$\frac{B_{1,1}(\lambda_1)}{B_{2d}} = 0.5652 \qquad or \qquad B_{1,1} = 1.3894 \ \ (tesla)$$
$$\frac{B_{1,1}(\lambda_2)}{B_{2d}} = 1.0518 \qquad or \qquad B_{1,1} = 2.5858 \ \ (tesla)$$

We comment here that the field components as described by Eq. (26) differs from the corresponding expression written in the Appendix of a paper by J.Blewett et al[d] due to possible typographical errors in that paper. We also note that if we express the total current written in equation (31) in a form similar to that expressed in Blewett's paper we arrive at the total current per pole (= $2I_0$)

$$Current/pole = \frac{5 B_{1,1}\lambda_0}{\pi^2(\frac{\pi R}{L}K_0 + K_1)} \tag{39}$$

where λ_0=2L (period). Blewett's expression for the current differs by a factor of $\sqrt{1 + (\frac{L}{\pi R})^2}$

$$Current/pole = \frac{5 B_{1,1}\lambda_0 \sqrt{1 + (\frac{L}{\pi R})^2}}{\pi^2(\frac{\pi R}{L}K_0 + K_1)} \tag{40}$$

For the case of a single pair of current carrying wires wound in a bifilar helix[e] this expression is also different from both cases.

$$Current/pole = \frac{5 B_{1,1}\lambda_0}{4\pi(\frac{\pi R}{L}K_0 + K_1)} \tag{41}$$

d Orbits and fields in the helical wiggler — Journal of Applied Physics, Vol. 48, No. 7, July 1977

e Static and Dynamic Electricity — W.R.Smythe, p.277.

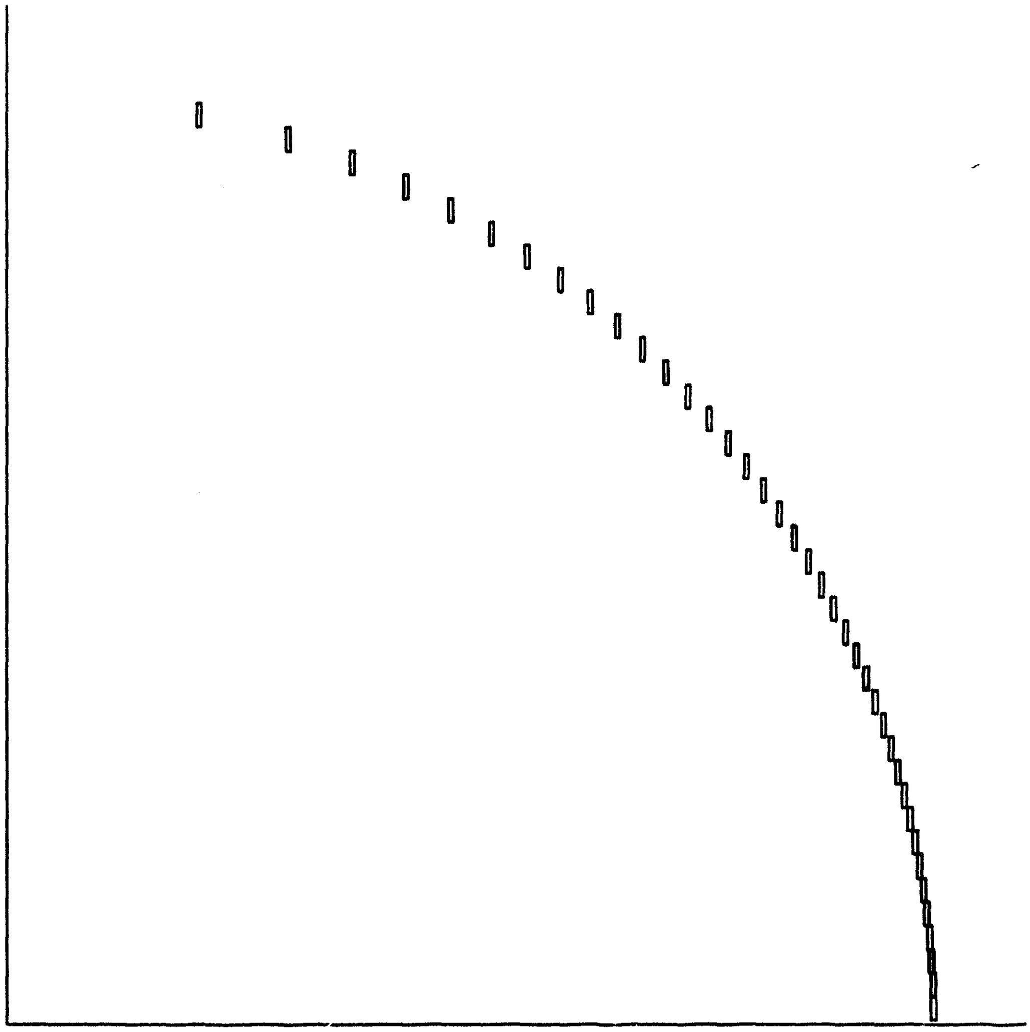

Figure 2 Winding cross section in a cosθ configuration.

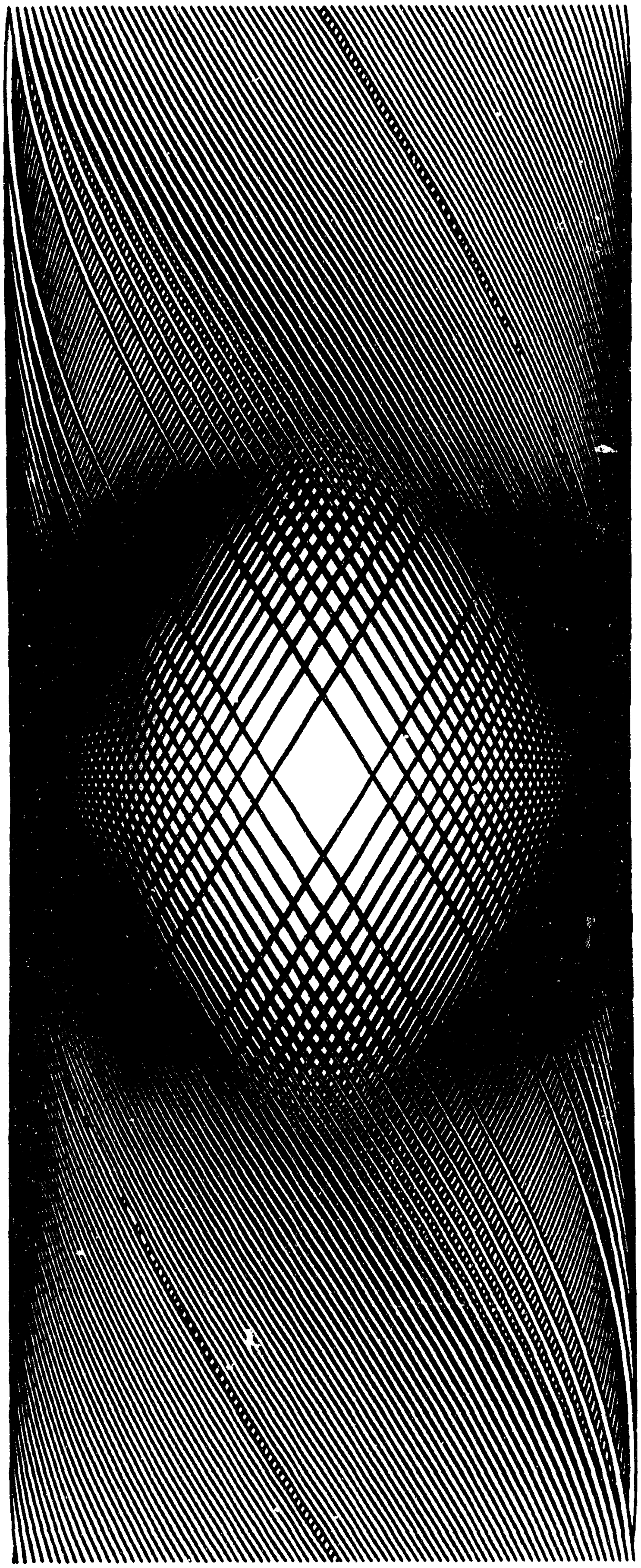

Figure 3 3D windings for half period L=10 in a $\cos(\pi z/L)$ configuration.

Appendix A Iron contribution

Equation (22) suggest a field enhancement factor arising from an iron sheet placed at r=a. Figure 4 shows such a factor for n=1 and m=1 as a function of $s = \frac{\pi R}{L}$ with the ratio of a/R used as a parameter.[f]

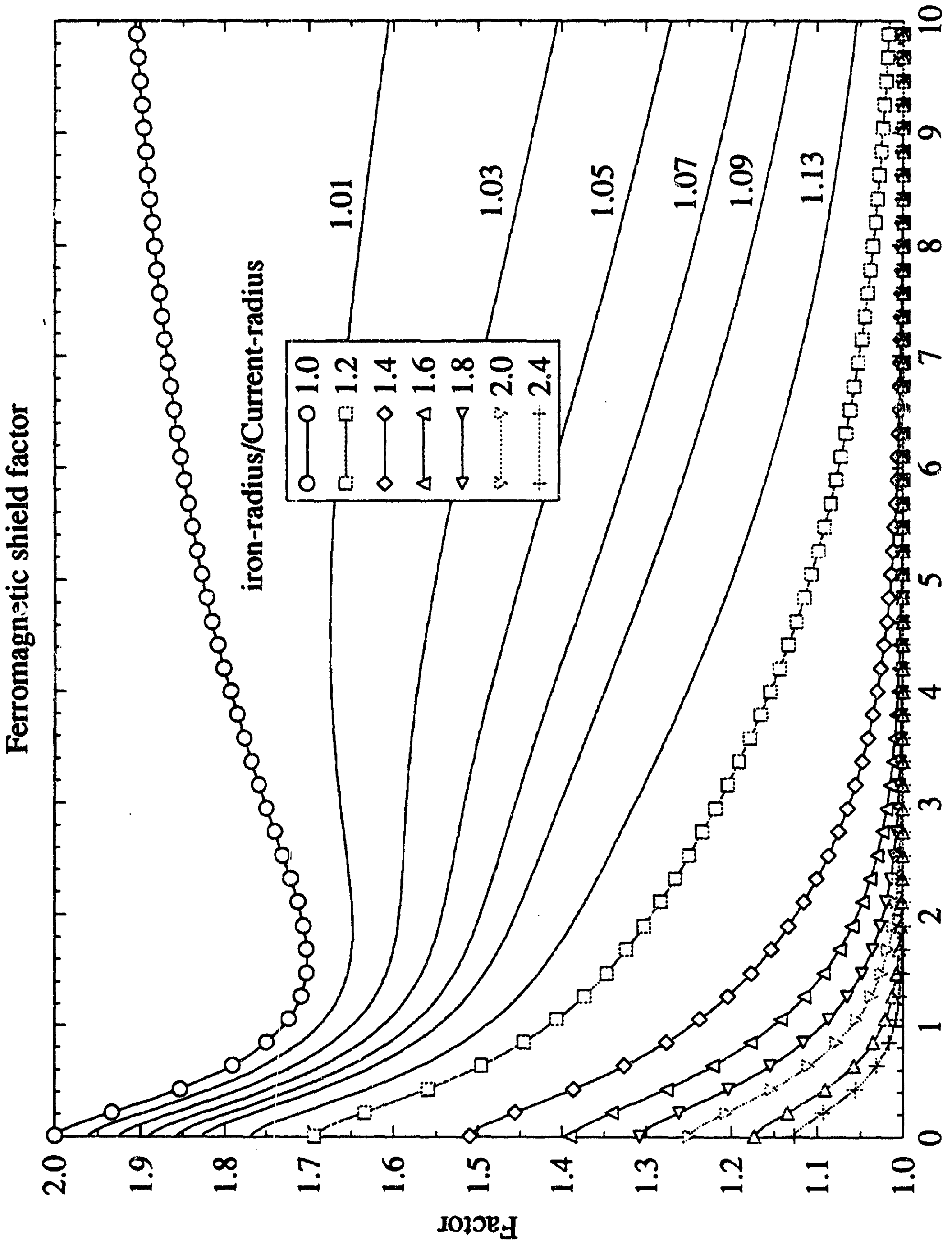

Figure 4 Field compression factor in a helical dipole wiggler.

[f] I would like to acknowledge the help I received from Domenico Dell'orco in producing this graph.

Appendix B 3D harmonic coefficients

In order that the series for the potential V_n satisfy the differential equation (Eq. 1) we introduce the functions $A_n(z)$ and express the coefficients g_{rn} , $g_{\theta n}$,g_{zn} as general functions of r and z as shown below :

$$
\begin{aligned}
g_{rn}(r,z) &= \sum_{k=0} (-1)^{k+1} \frac{n!(n+2k)}{2^{2k}k!(n+k)!} A_n^{(2k)}(z) r^{2k} \\
g_{\theta n}(r,z) &= \sum_{k=0} (-1)^{k+1} \frac{n!n}{2^{2k}k!(n+k)!} A_n^{(2k)}(z) r^{2k} \\
g_{zn}(r,z) &= \sum_{k=0} (-1)^{k+1} \frac{n!}{2^{2k}k!(n+k)!} A_n^{(2k+1)} r^{2k}
\end{aligned} \tag{1}
$$

Explicitly we can write the above as :

$$
\begin{aligned}
g_{rn}(r,z) &= -nA_n(z) + \frac{n+2}{4(n+1)} A_n^{''}(z) r^2 - \frac{n+4}{32(n+1)(n+2)} A_n^{''''}(z) r^4 \\
&\quad + \frac{n+6}{384(n+1)(n+2)(n+3)} A_n^{''''''}(z) r^6 - \dots \\
g_{\theta n}(r,z) &= -nA_n(z) + \frac{n}{4(n+1)} A_n^{''}(z) r^2 - \frac{n}{32(n+1)(n+2)} A_n^{''''}(z) r^4 \\
&\quad + \frac{n}{384(n+1)(n+2)(n+3)} A_n^{''''''}(z) r^6 - \dots \\
g_{zn}(r,z) &= -A_n^{'}(z) + \frac{1}{4(n+1)} A_n^{'''}(z) r^2 - \frac{1}{32(n+1)(n+2)} A_n^{'''''}(z) r^4 \dots\dots
\end{aligned} \tag{2}
$$

For the expressions of the skew terms just replace g_{rn} , $g_{\theta n}$,g_{zn} with $\tilde{g}_{rn}$, $\tilde{g}_{\theta n}$,$\tilde{g}_{zn}$ and $A_n(z)$ with $\tilde{A}_n(z)$

The representation specified above for 3–D magnetic fields, can be written in terms of functions $A_n(z)$ and $\tilde{A}_n(z)$ and their derivatives for the example used in the main part of the paper where n=1 and m=1, such that :

$$
\begin{aligned}
A_1^{(2k)} &= (-1)^k \left(\frac{\pi}{L}\right)^{2k} B_{1,1} \cos\frac{\pi z}{L} \\
\tilde{A}_1^{(2k)} &= (-1)^k \left(\frac{\pi}{L}\right)^{2k} B_{1,1} \sin\frac{\pi z}{L} \\
A_1^{(2k-1)} &= (-1)^k \left(\frac{\pi}{L}\right)^{2k-1} B_{1,1} \sin\frac{\pi z}{L} \\
\tilde{A}_1^{(2k-1)} &= (-1)^{k+1} \left(\frac{\pi}{L}\right)^{2k-1} B_{1,1} \cos\frac{\pi z}{L}
\end{aligned} \tag{3}
$$

In the next series of graphs we include results of such A's (both normal and skew) computed by the program "figends" for one of the example previously noted (2L=5.0). We note the sinusoidal periodicity of the A's and their derivatives according to the above relations.

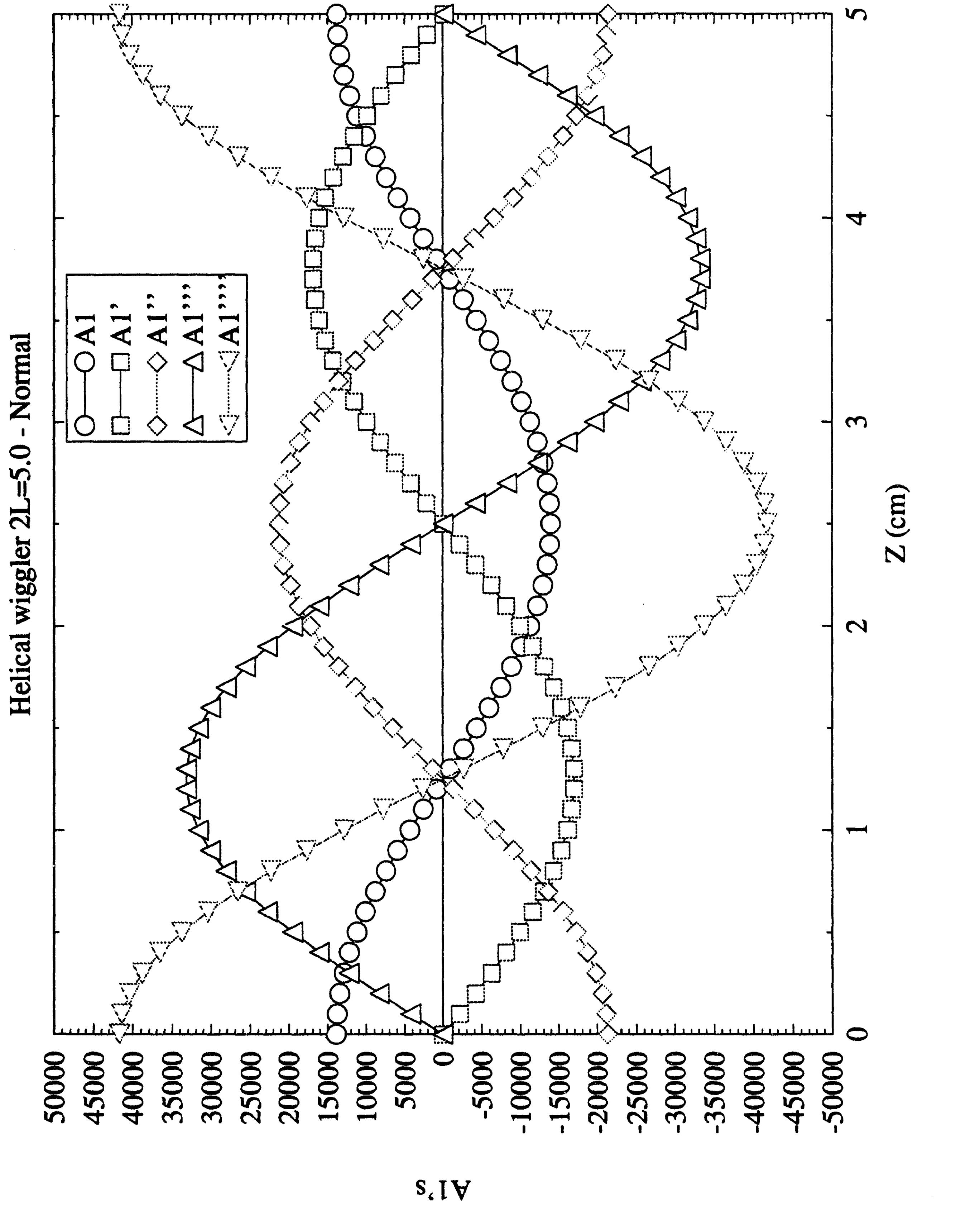

Figure 6 Normal A1 as a function of z over a full period..

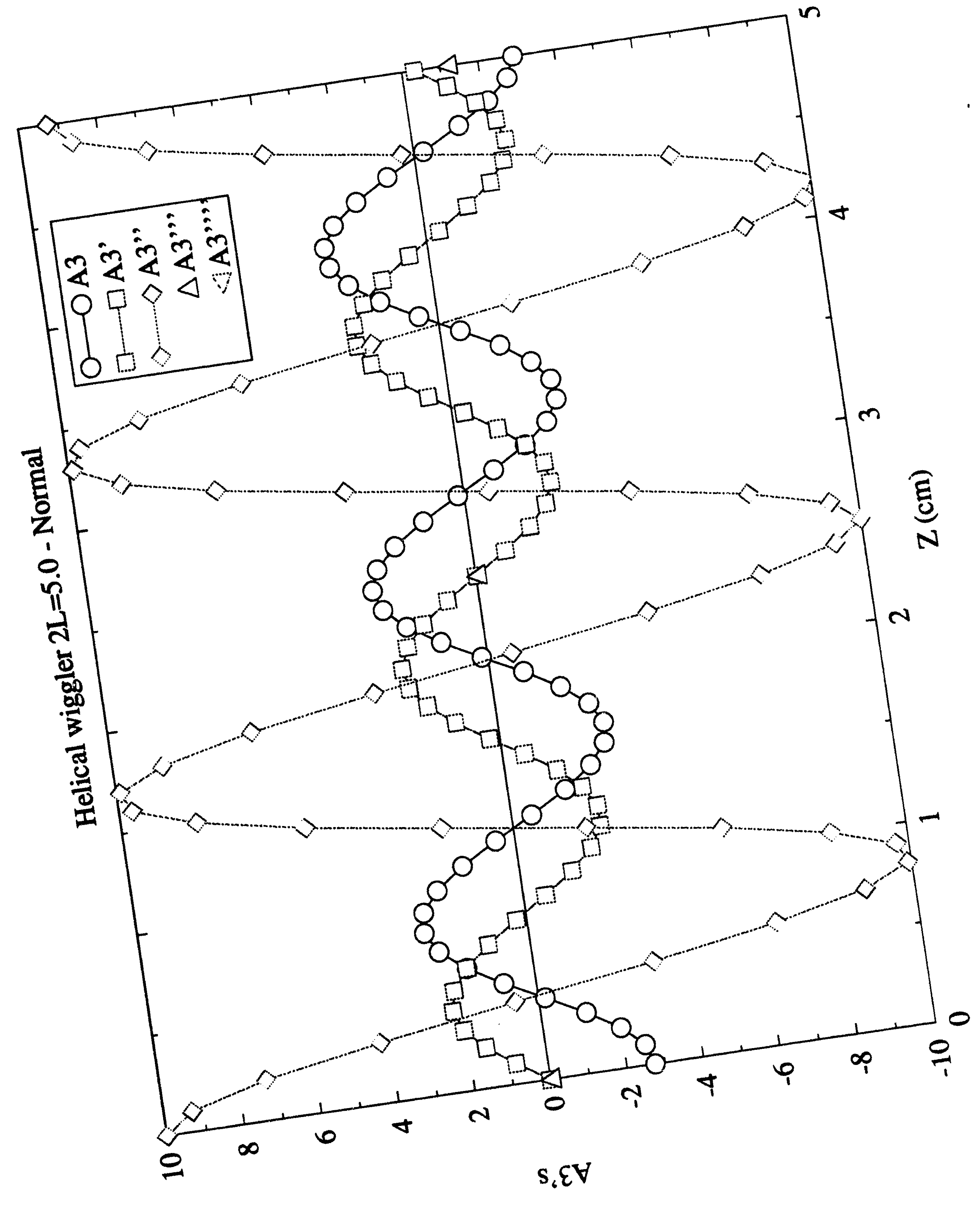

Figure 7 Normal A3 as a function of z over a full period..

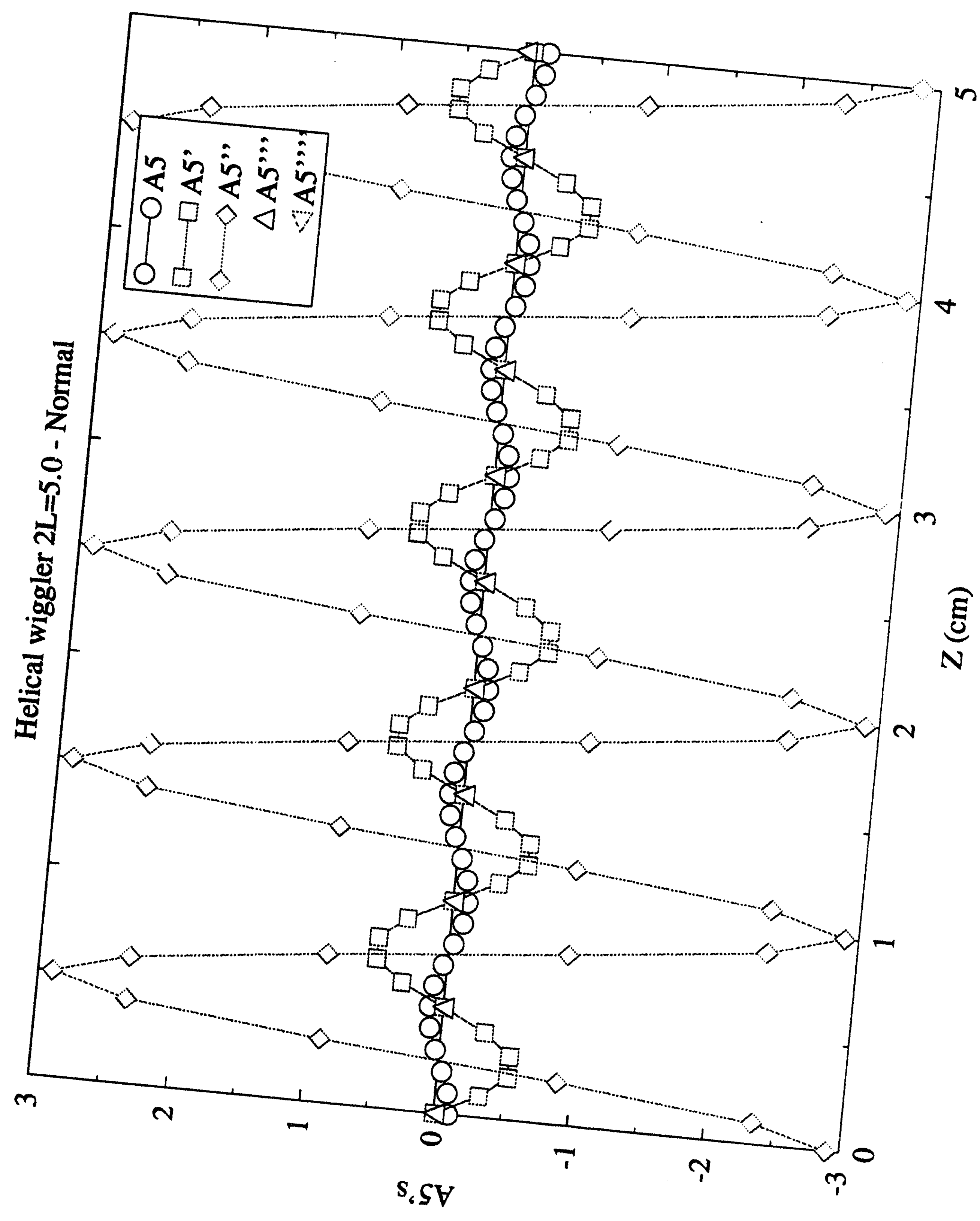

Figure 8 Normal A5 as a function of z over a full period..

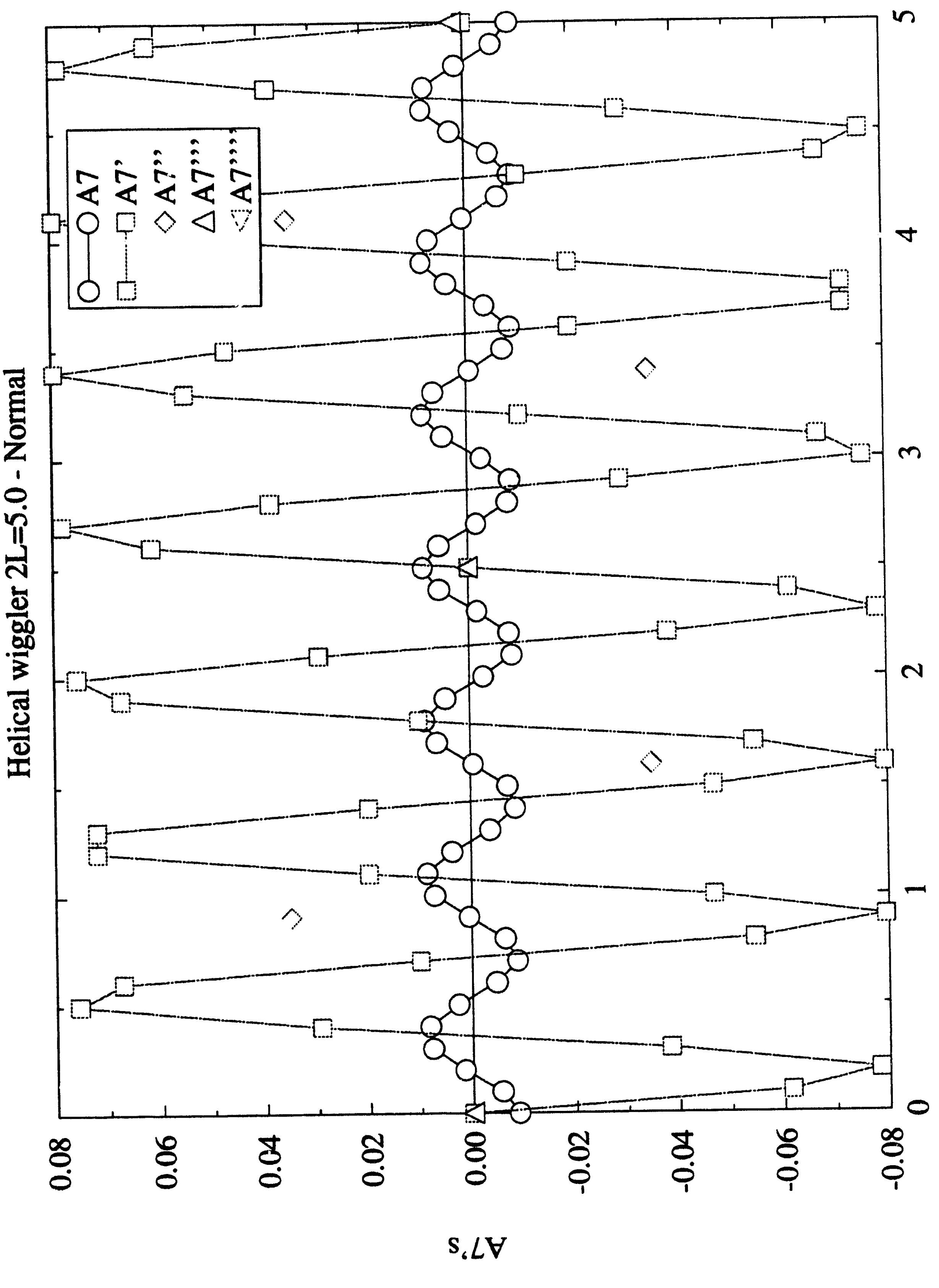

Figure 9 Normal A7 as a function of z over a full period..

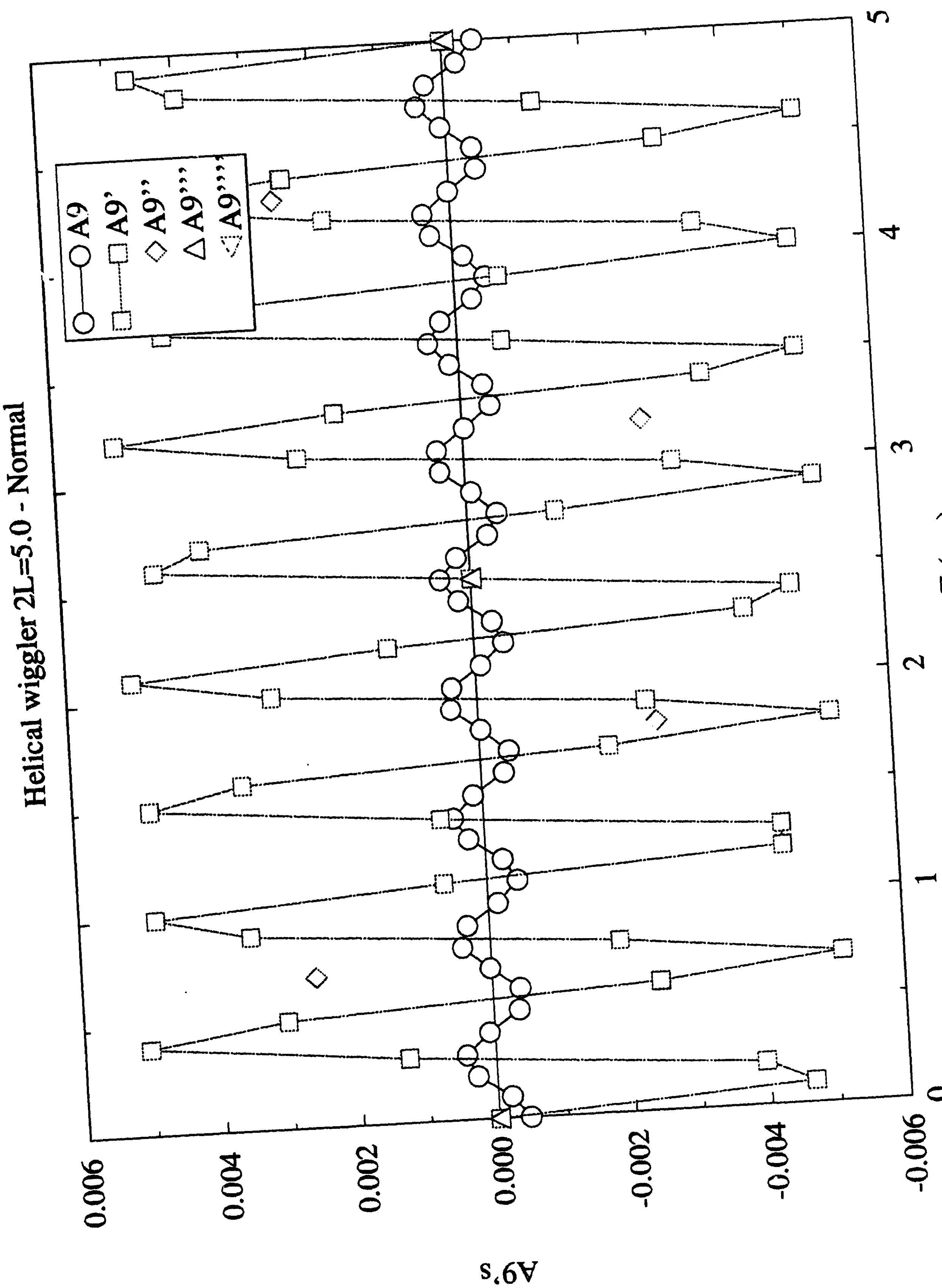

Figure 10 Normal A9 as a function of z over a full period..

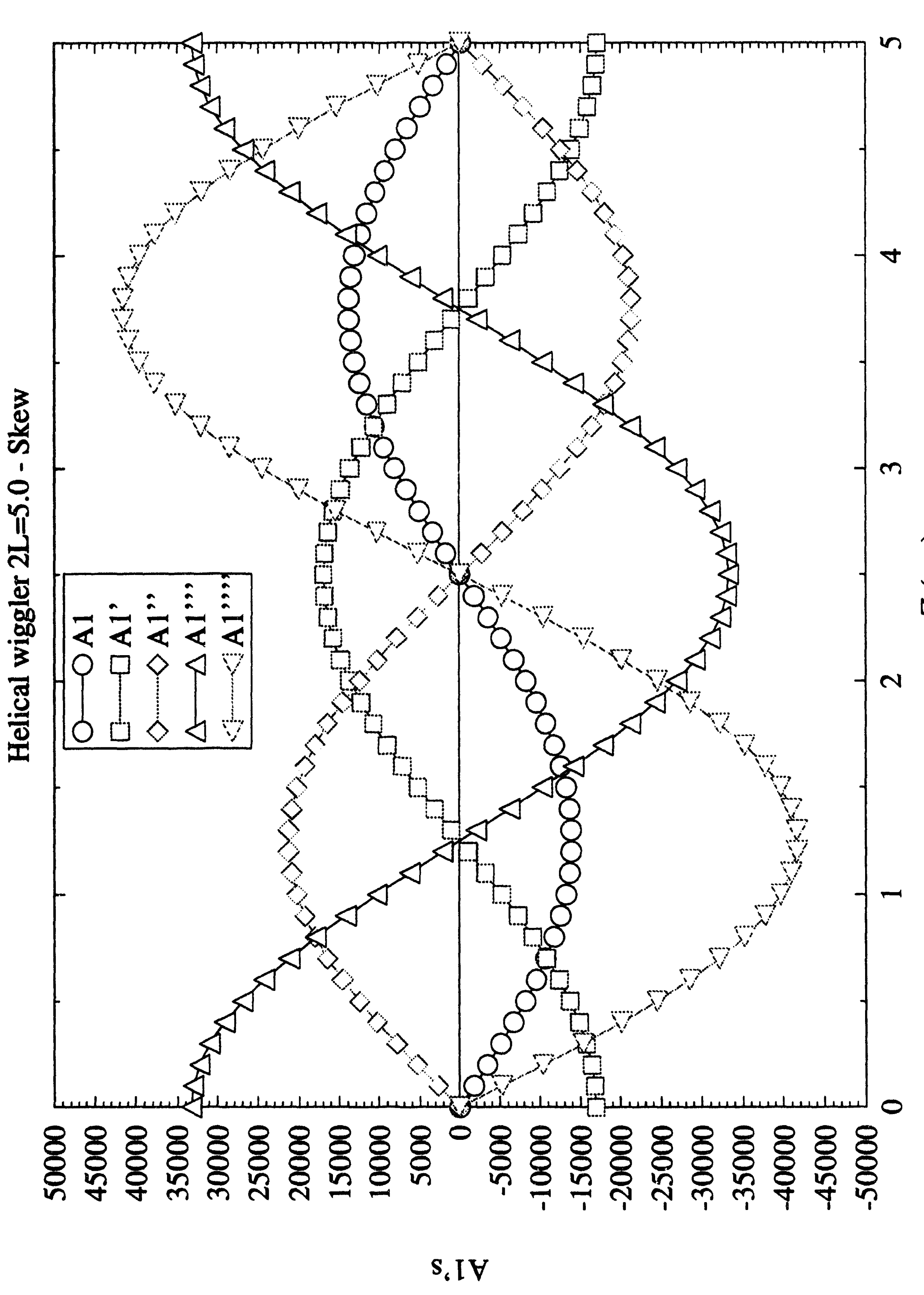

Figure 11 Skew A1 as a function of z over a full period..

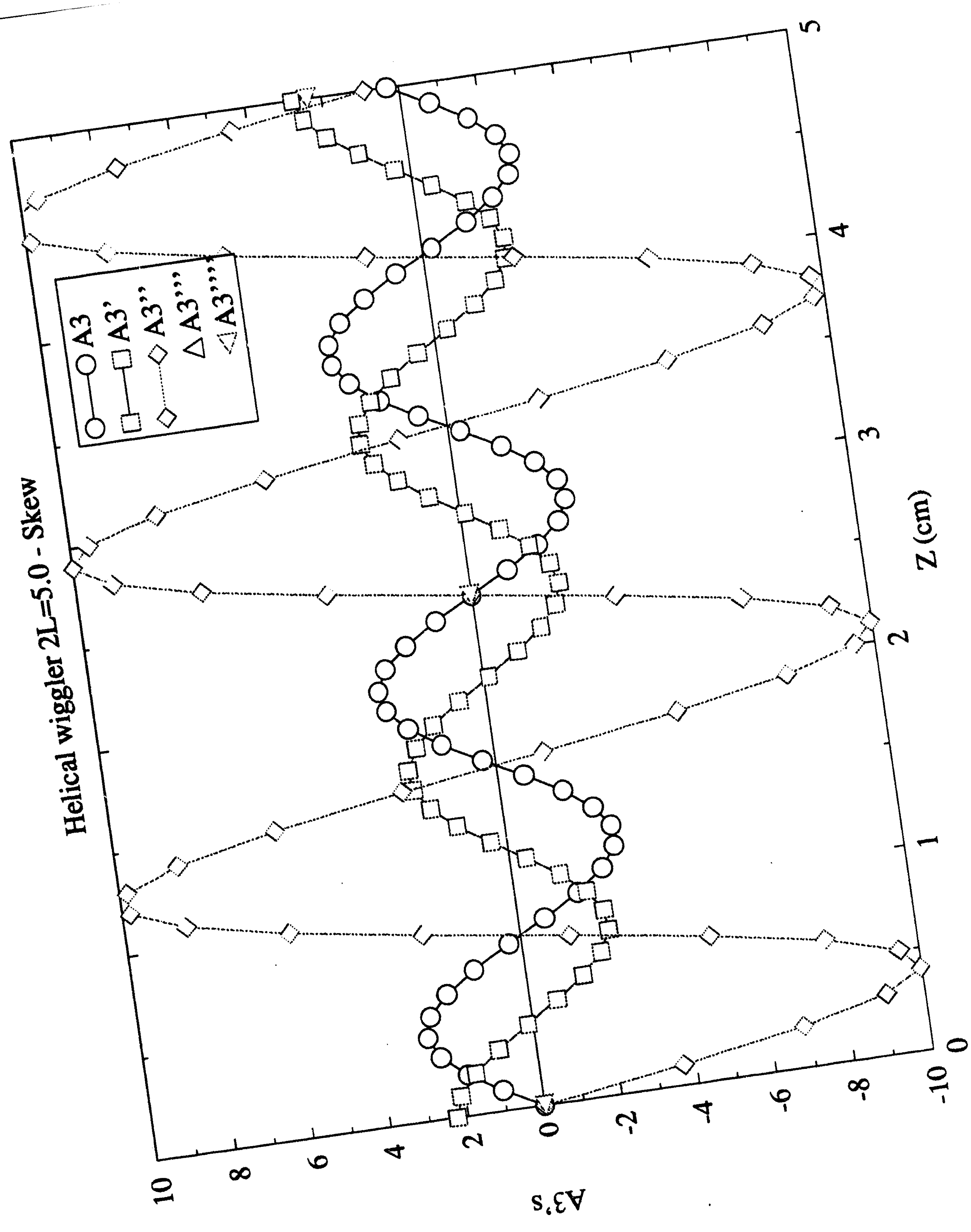

Figure 12 Skew A3 as a function of z over a full period..

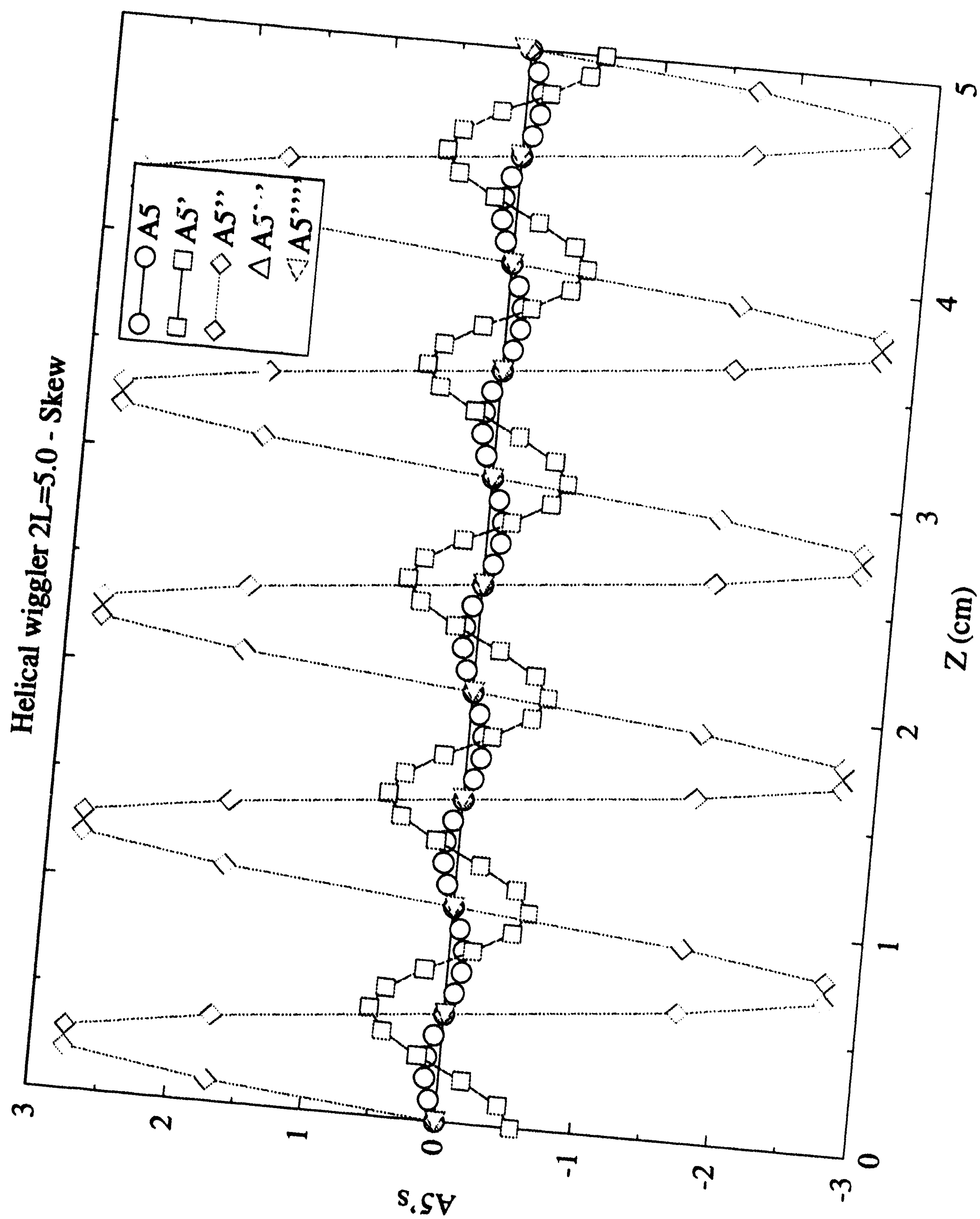

Figure 13 Skew A5 as a function of z over a full period..

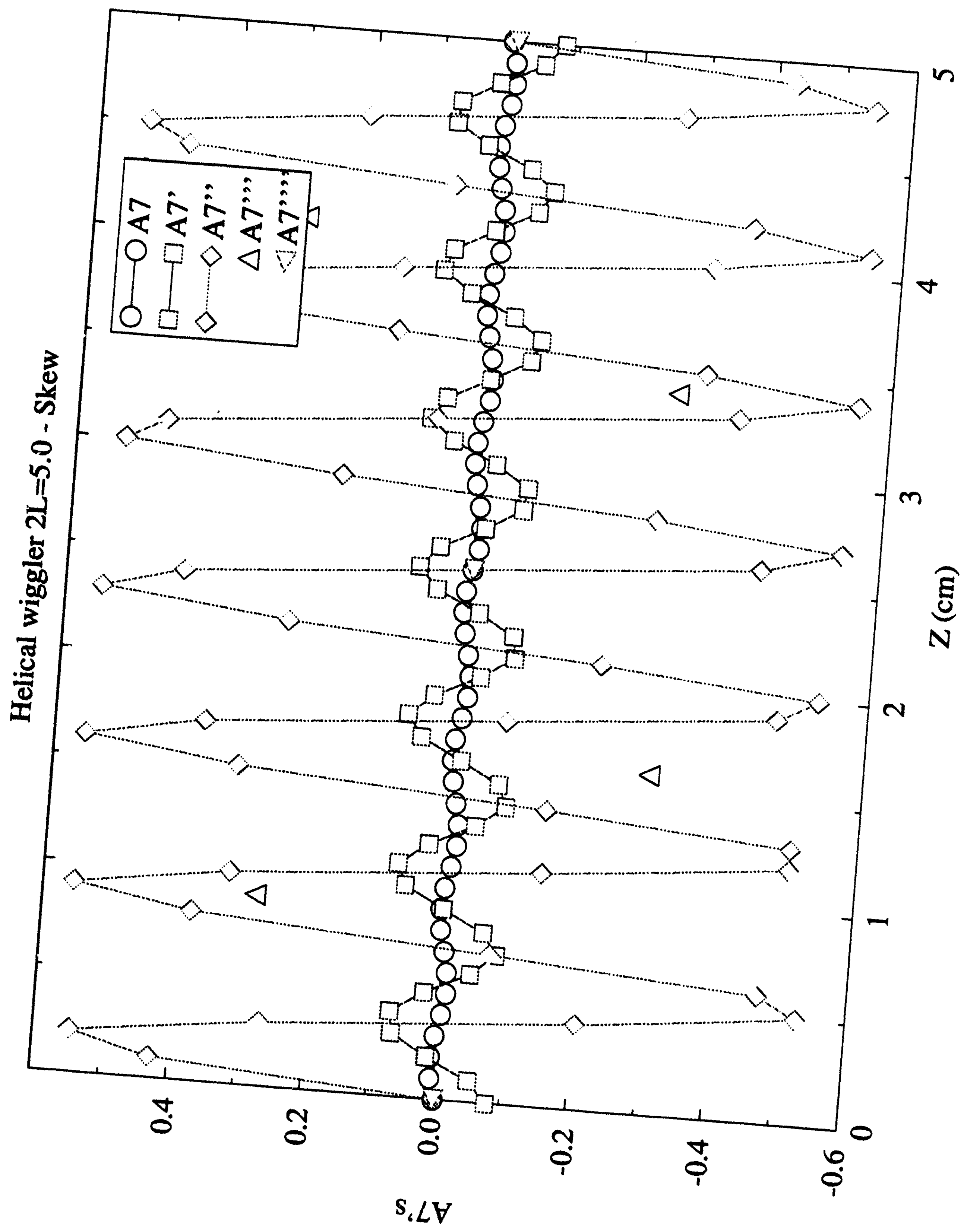

Figure 14 Skew A7 as a function of z over a full period..

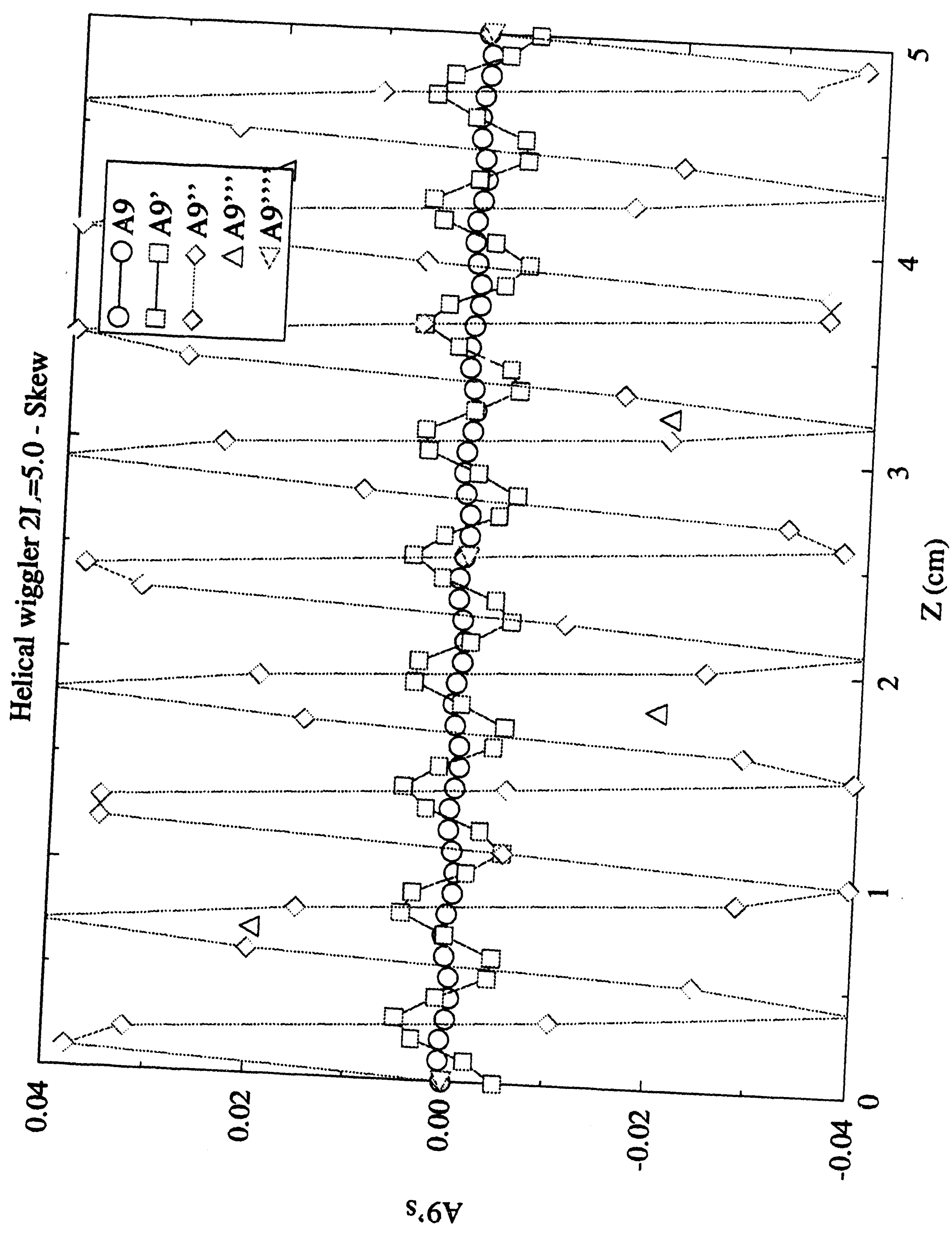

Figure 15 Skew A9 as a function of z over a full period..

DATE
FILMED
10/19/94

END